

Coverage Analysis of Finite Cellular Networks: A Stochastic Geometry Approach

Seyed Mohammad Azimi-Abarghouyi*, Behrooz Makki[†], Martin Haenggi[‡], Masoumeh Nasiri-Kenari*,
and Tommy Svensson[†]

*Sharif University of Technology, Tehran, Iran, [†]Chalmers University of Technology, Gothenburg, Sweden,

[‡]University of Notre Dame, IN, USA

Abstract—This paper develops a tractable modeling and analysis framework for finite cellular wireless networks using stochastic geometry. Defining finite homogeneous Poisson point processes to model the number and locations of access points in a confined region, we study the coverage probability for an arbitrarily-located reference user that is served by the closest access point. The distance distribution and the Laplace transform (LT) of the interference are derived. We also derive a closed-form lower bound on the LT of the interference. Our analyses reveal that a higher path loss exponent improves the coverage probability and that there is a location where the coverage probability is maximized.

I. INTRODUCTION

Finite wireless networks are composed of a number of nodes randomly distributed inside a region with finite size. This spatial setup is a useful model for millimeter wave communications, indoor, and ad hoc networks as candidate technologies for emerging 5G wireless networks [1]. This setup is also appropriate in applications where there is a range limit for backhaul links, e.g., cloud radio access networks [2]. Also, the ever-increasing randomness in the locations of nodes in a wireless network has led to a growing interest in the use of stochastic geometry and Poisson point processes (PPPs) for accurate and tractable spatial modeling and analysis [3].

The stochastic geometry-based modeling and analysis of finite wireless networks is more challenging and requires different approaches than wireless networks over infinite regions that are often modeled by the infinite homogeneous PPP (HPPP) [4, Def. 2.8]. The main challenge is that a finite point process is not statistically similar at different locations, and consequently, the performance is location-dependent. Using the binomial point process (BPP) [4, Def. 2.11], finite wireless networks have been well studied, e.g., [5]-[8]. In the BPP model, a fixed number of nodes are distributed independently and uniformly inside a finite region. Considering a disk, [5] has developed a comprehensive framework for performance characterizations of an arbitrarily-located reference user under different selection strategies. Disk-shaped networks of unmanned aerial vehicles are analyzed in [6]. There are also studies that present performance characterizations of a fixed link inside an arbitrarily-shaped finite region [7]-[8].

In this paper, we develop a tractable model for finite cellular wireless networks, where a reference user is served by the closest access point. We define a finite homogeneous Poisson point process (FHPPP) to model access points in a finite

region and then derive an exact expression for the coverage probability. As a key step for the coverage probability analysis, we characterize the Laplace transform (LT) of the interference and the distribution of the distance from the reference user to its serving access point. We also derive a tight closed-form lower bound on the LT of the interference that requires much less numerical computations.

Our work is different from the state-of-the-art literature on finite networks, e.g., [5]-[8], since different from the BPP, which models a fixed number of nodes in a region, we consider a point process that is suitable for finite regions with a random number of nodes and allow for arbitrary user locations.

The rest of the paper is organized as follows. Section II describes the system model. Section III characterizes the serving distance distribution. Section IV presents the analytical result for the coverage probability, and derives the LT of the interference. Section V derives the lower bound on the coverage probability. Section VI presents the numerical results. Finally, Section VII concludes the paper.

II. SYSTEM MODEL

In this section, we present a mathematical model of the system. We begin with the spatial distribution of the nodes. Then, we describe the channel model and define the signal-to-interference-and-noise ratio (SINR).

A. Spatial Model

Let us define an FHPPP as follows.

Definition 1: We define the FHPPP as $\Phi = \mathcal{P} \cap \mathcal{A}$, where \mathcal{P} is an HPPP of intensity λ and $\mathcal{A} \subset \mathbb{R}^2$. ■

We consider a finite cellular network as shown in Fig. 1, where the locations of active access points are modeled as an FHPPP. For simplicity and in harmony with, e.g., [5]-[6], we let $\mathcal{A} = \mathbf{b}(\mathbf{x}_o, D)$, where $\mathbf{b}(\mathbf{x}_o, D)$ represents a disk centered at \mathbf{x}_o with radius D . However, our theoretical results can be extended to an arbitrarily-shaped region \mathcal{A} .

Users can be located anywhere in \mathbb{R}^2 . With no loss of generality, we conduct the analysis at a reference user located at the origin \mathbf{o} . We further define $d = \|\mathbf{x}_o\|$, which denotes the distance from the reference user to the center of \mathcal{A} .¹

¹The locations of the reference user and the center of \mathcal{A} can be anywhere in \mathbb{R}^2 . The origin \mathbf{o} and \mathbf{x}_o are relatively determined in a coordinate system.

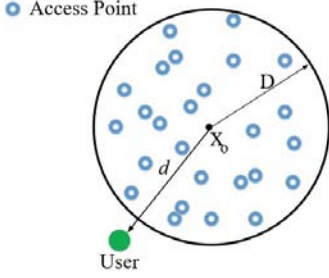


Fig. 1: An illustration of finite cellular wireless networks.

B. Channel Model and SINR

We assume distance-dependent power-law path loss and Rayleigh fading. Thus, the received power at the reference user from an access point located at \mathbf{y} is $h_{\mathbf{y}}\|\mathbf{y}\|^{-\alpha}$, where the transmit power is set to 1 with no loss of generality and $\alpha > 2$ is the path loss exponent. The sequence $\{h_{\mathbf{y}}\}$ consists of i.i.d. exponential random variables with mean 1.

The SINR of the reference user can be expressed as

$$\text{SINR}_c = \frac{h_{\mathbf{x}_c}\|\mathbf{x}_c\|^{-\alpha}}{\sigma^2 + \mathcal{I}_c}, \quad (1)$$

where \mathbf{x}_c is the location of the serving access point, $\mathcal{I}_c = \sum_{\mathbf{y} \in \Phi \setminus \{\mathbf{x}_c\}} h_{\mathbf{y}}\|\mathbf{y}\|^{-\alpha}$ denotes the interference, and σ^2 is the noise power. For notational simplicity, we define the serving distance as $R_c = \|\mathbf{x}_c\|$.

III. SERVING DISTANCE DISTRIBUTION

In this section, we derive the distribution of the distance from the reference user to its serving access point. This distance distribution will be used later in the coverage probability analysis.

Let us first define $\varphi_0 = \sin^{-1}\left(\frac{D}{d}\right)$, $\varphi_1(r) = \cos^{-1}\left(\frac{r^2 + d^2 - D^2}{2dr}\right)$, $R_1(\theta) = d \cos(\theta) + \sqrt{D^2 - d^2 \sin^2(\theta)}$ and $\hat{R}_1(\theta) = d \cos(\theta) - \sqrt{D^2 - d^2 \sin^2(\theta)}$, and present a lemma on the intersection area of two circles.

Lemma 1: Consider two circles with radii D and r_c with centers separated by distance d . The area of their intersection is given by [9, Eq. (12.76)]

$$\mathcal{B}_d(r_c) = D^2 \cos^{-1}\left(\frac{D^2 + d^2 - r_c^2}{2dD}\right) + r_c^2 \varphi_1(r_c) - \frac{1}{2} \sqrt{[(r_c + d)^2 - D^2][D^2 - (r_c - d)^2]}. \quad (2)$$

The distance from the reference user to its closest access point R_c is larger than r_c if and only if at least one access point

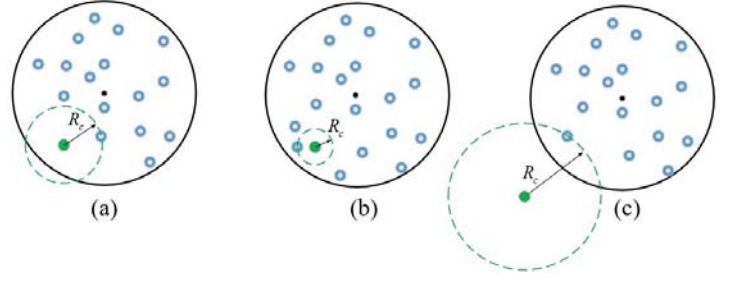


Fig. 2: An illustration of the intersection in the case $d \leq D$ for Subplot (a): $D - d \leq R_c < D + d$ and Subplot (b): $0 \leq R_c < D - d$, and in the case $d > D$ for Subplot (c): $d - D \leq R_c < d + D$.

exists inside \mathcal{A} and there is no access point located within $\mathbf{b}(\mathbf{o}, r_c) \cap \mathcal{A}$. Letting \mathcal{C}_{r_c} denote the intersection, we have

$$\begin{aligned} \mathbb{P}(R_c > r_c) &= \frac{\mathbb{P}(n(\Phi \cap \mathcal{C}_{r_c}) = 0 \text{ and } n(\Phi) > 0)}{\mathbb{P}(n(\Phi) > 0)} \\ &\stackrel{(a)}{=} \frac{\mathbb{P}(n(\Phi \cap \mathcal{C}_{r_c}) = 0) \mathbb{P}(n(\Phi \setminus \mathcal{C}_{r_c}) > 0)}{\mathbb{P}(n(\Phi) > 0)} \\ &\stackrel{(b)}{=} \frac{\exp(-\lambda |\mathcal{C}_{r_c}|) (1 - \exp(-\lambda(\pi D^2 - |\mathcal{C}_{r_c}|)))}{1 - \exp(-\lambda \pi D^2)} \\ &= \frac{\exp(-\lambda |\mathcal{C}_{r_c}|) - \exp(-\lambda \pi D^2)}{1 - \exp(-\lambda \pi D^2)}, \end{aligned} \quad (3)$$

where $|\mathcal{C}_{r_c}|$ denotes the area of \mathcal{C}_{r_c} . Also, (a) is due to the fact that the numbers of points of a PPP in disjoint regions are independent, and (b) is because $R_c \leq D + d$.

According to Fig. 2, there are two different cases for $|\mathcal{C}_{r_c}|$ as follows.

Case 1: If $d \leq D$, then

$$|\mathcal{C}_{r_c}| = \begin{cases} \pi r_c^2 & 0 \leq r_c < D - d, \\ \mathcal{B}_d(r_c) & D - d \leq r_c < D + d, \\ \pi D^2 & r_c \geq D + d, \end{cases} \quad (4)$$

where $\mathcal{B}_d(r_c)$ is given in (2).

Case 2: If $d > D$, then

$$|\mathcal{C}_{r_c}| = \begin{cases} 0 & 0 \leq r_c < d - D, \\ \mathcal{B}_d(r_c) & d - D \leq r_c < D + d, \\ \pi D^2 & r_c \geq D + d. \end{cases} \quad (5)$$

IV. COVERAGE PROBABILITY

In this section, we derive the coverage probability of the reference user. As a key step in the coverage probability analysis, we obtain the LT of the interference (Theorem 1). For notational simplicity, we define $\mathcal{F}(s, x) = x^2 {}_2F_1\left(1, \frac{2}{\alpha}; 1 + \frac{2}{\alpha}; -\frac{1}{s} x^\alpha\right)$ where ${}_2F_1(a, b; c; t)$ denotes the Gauss hypergeometric function [10].

Theorem 1: Conditioned on R_c , the LT of the interference is

$$\mathcal{L}_{\mathcal{I}_c}^d(s|R_c) = \exp\left(\pi \lambda \mathcal{F}(s, R_c) - \lambda \int_0^\pi \mathcal{F}(s, R_1(\theta)) d\theta\right), \quad (6)$$

if $d \leq D$ and $0 \leq R_c < D - d$, and

$$\begin{aligned} &\blacksquare \mathcal{L}_{\mathcal{I}_c}^d(s|R_c) = \\ &\exp\left(\varphi_1(R_c) \lambda \mathcal{F}(s, R_c) - \lambda \int_0^{\varphi_1(R_c)} \mathcal{F}(s, R_1(\theta)) d\theta\right), \end{aligned} \quad (7)$$

if $d \leq D$ and $D - d \leq R_c < D + d$ or $d > D$ and $\sqrt{d^2 - D^2} \leq R_c < d + D$, and

$$\begin{aligned} \mathcal{L}_{\mathcal{I}_c}^d(s|R_c) = & \\ \exp\left(\varphi_1(R_c)\lambda\mathcal{F}(s, R_c) - \lambda \int_0^{\varphi_1(R_c)} \mathcal{F}(s, R_1(\theta))d\theta\right) \times & \\ \exp\left(-\lambda \int_{\varphi_1(R_c)}^{\varphi_0} \left\{\mathcal{F}(s, R_1(\theta)) - \mathcal{F}(s, \hat{R}_1(\theta))\right\}d\theta\right), & \quad (8) \end{aligned}$$

if $d > D$ and $d - D \leq R_c < \sqrt{d^2 - D^2}$. Also, φ_0 , φ_1 , R_1 and \hat{R}_1 are defined in Section III.

Proof: See Appendix A. \blacksquare

Using the conditional LT of the interference derived in Theorem 1, we can express the coverage probability of the reference user as

$$P_C^c(\beta) = \mathbb{P}(n(\Phi) > 0)\mathbb{P}(\text{SINR}_c > \beta \mid n(\Phi) > 0), \quad (9)$$

where β is the minimum required SINR for coverage. Note that the coverage probability is zero when there is no access point. Then, from (1) and averaging over the serving distance R_c , we have

$$P_C^c(\beta) = (1 - \exp(-\lambda\pi D^2)) \times \int_0^\infty \mathbb{P}\left(\frac{h_{\mathbf{x}_c} r_c^{-\alpha}}{\sigma^2 + \mathcal{I}_c} > \beta\right) f_{R_c}^d(r_c) dr_c, \quad (10)$$

where $f_{R_c}^d$ is the PDF of R_c obtained from (3). The conditional coverage probability given a serving distance r_c can be expressed as

$$\begin{aligned} \mathbb{P}\left(\frac{h_{\mathbf{x}_c} r_c^{-\alpha}}{\sigma^2 + \mathcal{I}_c} > \beta\right) &= \mathbb{P}(h_{\mathbf{x}_c} > \beta r_c^\alpha (\sigma^2 + \mathcal{I}_c)) \\ &\stackrel{(a)}{=} \mathbb{E}\left\{\exp(-\beta r_c^\alpha (\sigma^2 + \mathcal{I}_c))\right\} \\ &= \exp(-\beta\sigma^2 r_c^\alpha) \mathcal{L}_{\mathcal{I}_c}^d(\beta r_c^\alpha | r_c), \quad (11) \end{aligned}$$

where (a) follows from $h_{\mathbf{x}_c} \sim \exp(1)$. Finally, according to Section III and with $\mathcal{L}_{\mathcal{I}_c}^d$ given in (6)-(8), the coverage probability is obtained as

$$\begin{aligned} P_C^c(\beta) = & \\ \int_0^{D-d} 2\pi\lambda r_c \exp(-\lambda\pi r_c^2) \exp(-\beta\sigma^2 r_c^\alpha) \mathcal{L}_{\mathcal{I}_c}^d(\beta r_c^\alpha | r_c) dr_c & \\ + \int_{D-d}^{D+d} \lambda \frac{\partial \mathcal{B}_d(r_c)}{\partial r_c} \exp(-\lambda\mathcal{B}_d(r_c)) \exp(-\beta\sigma^2 r_c^\alpha) \times & \\ \mathcal{L}_{\mathcal{I}_c}^d(\beta r_c^\alpha | r_c) dr_c, & \quad (12) \end{aligned}$$

if $d \leq D$, and

$$P_C^c(\beta) = \int_{d-D}^{D+d} \lambda \frac{\partial \mathcal{B}_d(r_c)}{\partial r_c} \exp(-\lambda\mathcal{B}_d(r_c)) \times \exp(-\beta\sigma^2 r_c^\alpha) \mathcal{L}_{\mathcal{I}_c}^d(\beta r_c^\alpha | r_c) dr_c, \quad (13)$$

if $d > D$. In the special case of infinite cellular networks, i.e., $D \rightarrow \infty$, the coverage probability (13) simplifies to the result in [11, Thm. 2].

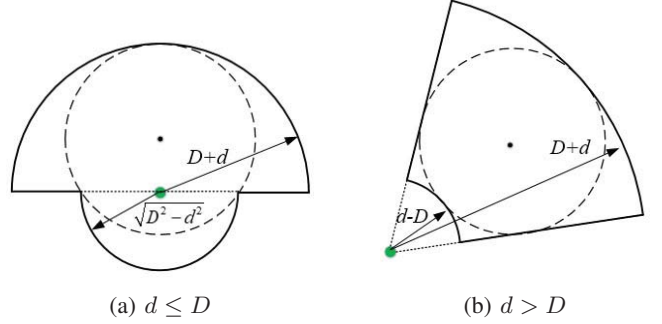


Fig. 3: Outer bounds of \mathcal{A} in the two cases $d \leq D$ and $d > D$.

V. LOWER BOUND ON COVERAGE PROBABILITY

Since the result derived for the LT of the interference in Theorem 1 requires intensive numerical computations, we derive a tight lower bound on the LT of the interference that is much easier to numerically evaluate. Then, inserting the bound in (12)-(13), a lower bound on coverage probability can be also provided. The tightness of the bound will be verified with numerical results (Fig. 6).

To obtain the lower bound, we outer bound the region \mathcal{A} by a region that permits a closed-form bound on the LT of the interference. Note that using a larger region leads to an upper bound on the interference, and therefore a lower bound on its LT.

The outer region for the cases with $d \leq D$ and $d > D$ is shown in Fig. 3. Locating the center of the sectors at the reference user in case $d \leq D$, two covering half-circles with radii $d + D$ and $\sqrt{D^2 - d^2}$ are considered. Also, in the case $d > D$, we consider the sector with radii $d + D$ and $d - D$ and the front angle $2\varphi_0$ entangled between the two tangent lines. However, in the case $d > D$, we can achieve a tighter bound by the following regions for $\mathcal{A} \setminus \mathbf{b}(\mathbf{o}, R_c)$, which is the region including interfering access points. In the case $R_c > \sqrt{d^2 - D^2}$, the sector with the front angle equal to twice the intersection angle, i.e., $2\varphi_1(R_c)$, and radii R_c and $D + d$ is considered. In the case $R_c < \sqrt{d^2 - D^2}$, we consider two sectors with the front angle $2\varphi_0$ and radii R_c and $R_1(\varphi_1(R_c))$ and with the front angle $2\varphi_1(R_c)$ and radii $R_1(\varphi_1(R_c))$ and $D + d$.

In the following corollary, we present the lower bound on the LT of the interference.

Corollary 1: Conditioned on R_c , the LT of the interference is lower bounded by

$$\begin{aligned} \mathcal{L}_{\mathcal{I}_{cb}}^d(s|R_c) = \exp\left(\pi\lambda\left\{\mathcal{F}(s, R_c) \right. \right. \\ \left. \left. - \frac{1}{2}\mathcal{F}(s, d+D) - \frac{1}{2}\mathcal{F}(s, \sqrt{D^2 - d^2})\right\}\right), \quad (14) \end{aligned}$$

if $d \leq D$ and $0 < R_c \leq \sqrt{D^2 - d^2}$, and

$$\mathcal{L}_{\mathcal{I}_{cb}}^d(s|R_c) = \exp\left(\frac{\pi}{2}\lambda\left\{\mathcal{F}(s, R_c) - \mathcal{F}(s, d+D)\right\}\right), \quad (15)$$

if $d \leq D$ and $\sqrt{D^2 - d^2} \leq R_c < D + d$, and

$$\begin{aligned} \mathcal{L}_{\mathcal{I}_{cb}}^d(s|R_c) = \exp\left(\lambda\left\{\varphi_0\mathcal{F}(s, R_c) + (\varphi_1(R_c) - \varphi_0) \times \right. \right. \\ \left. \left. \mathcal{F}(s, R_1(\varphi_1(R_c))) - \varphi_1(R_c)\mathcal{F}(s, d+D)\right\}\right), \quad (16) \end{aligned}$$

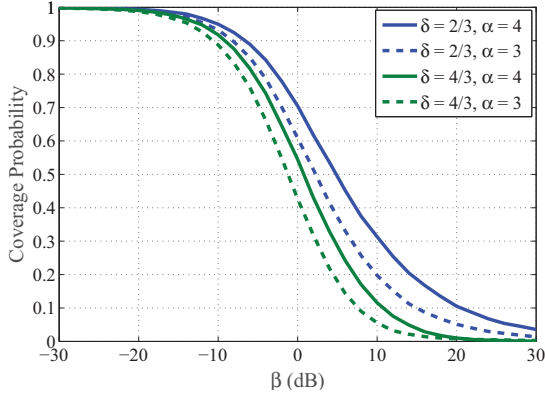


Fig. 4: Coverage probability as a function of the SINR threshold β .

if $d > D$ and $d - D \leq R_c < \sqrt{d^2 - D^2}$, and

$$\mathcal{L}_{\mathcal{I}_{cb}}^d(s|R_c) = \exp\left(\lambda\varphi_1(R_c)\left\{\mathcal{F}(s, R_c) - \mathcal{F}(s, d+D)\right\}\right), \quad (17)$$

if $d > D$ and $\sqrt{d^2 - D^2} \leq R_c < D + d$.

Proof: The proof follows the same approach as in Appendix A, except that the disk is replaced with the regions given in Fig. 3. ■

VI. NUMERICAL RESULTS

We consider a scenario of finite cellular wireless networks where the access points are distributed according to an FHPPP with intensity $\lambda = 0.01 \text{ m}^{-2}$ in a disk with radius $D = 15 \text{ m}$ and evaluate the coverage probability result derived in Section IV. We further define the normalized distance $\delta = \frac{d}{D}$. In the following, we investigate the impact of the path loss exponent and the distance of the user from the center of the disk on the coverage probability. We also study the tightness of the bound derived in Section V.

Effect of path loss exponent: The coverage probability as a function of the minimum required SINR β is plotted in Fig. 4 for $\delta = \frac{2}{3}$ and $\frac{4}{3}$ and $\alpha = 3$ and 4. It is observed that the coverage probability is improved when the path loss exponent is larger. That is because the power of both the desired and the interfering signals decrease as α increases, which can lead to an increase in the SINR.

Effect of user distance from the center: The coverage probability as a function of the normalized distance δ is studied in Fig. 5 for $\alpha = 4$ and $\beta = -5$ and 0 dB. It is observed that, depending on β , there is an optimal value for the distance of the user, about $0.8D$, in terms of the coverage probability. This is due to the fact that the SINR has a tradeoff since the power of both the desired and the interfering signals decrease as the distance of the user to the center of the disk increases.

Tightness of the bound: The tightness of the bound on coverage probability derived in Section V is evaluated in Fig. 6 for $\alpha = 4$ and $\delta = \frac{2}{3}$ and $\frac{4}{3}$. As observed, the bound tightly approximates the performance in a broad range of SINR thresholds β and for different positions of the user inside and outside the disk.

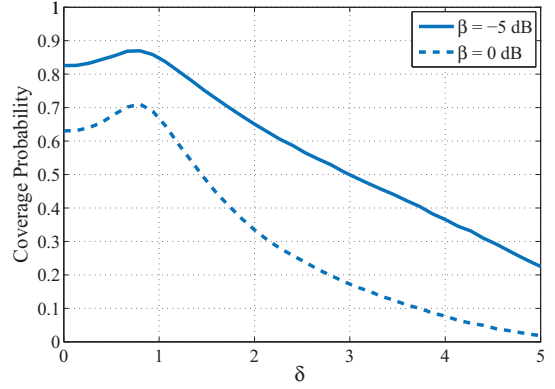


Fig. 5: Coverage probability as a function of normalized distance δ with $\alpha = 4$.

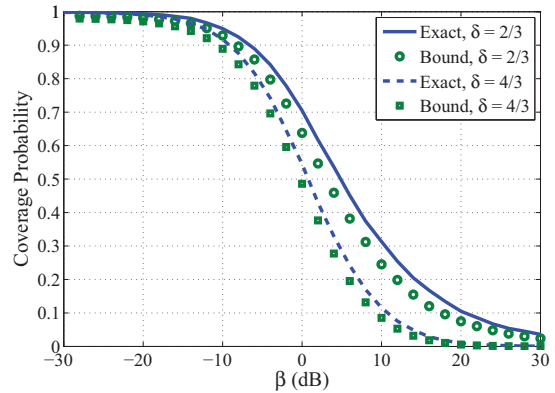


Fig. 6: On the tightness of the coverage probability lower bounds with $\alpha = 4$.

VII. CONCLUSION

In this paper, using stochastic geometry, we developed a tractable framework for the modeling and analysis of cellular wireless networks whose access points are located inside a finite region. We derived an exact expression for the coverage probability. We also proposed a tight closed-form expression bounding the coverage probability. Our analysis revealed that a higher path loss exponent improves the coverage probability. In addition, although an increase in the distance of the user to the center of finite region typically degrades the coverage probability, there exists a location where the coverage probability is maximized.

VIII. ACKNOWLEDGEMENT

This work has been supported by the Research Office of Sharif University of Technology under grant QB960605 and by the VR Research Link Project "Green Communications" and by the U.S. National Science Foundation under grant CCF 1525904.

APPENDIX A
PROOF OF THEOREM 1

Conditioned on the serving distance R_c , the LT of the interference is obtained as

$$\begin{aligned}
& \mathcal{L}_{\mathcal{I}_c}^d(s|R_c) \\
&= \mathbb{E} \left\{ \exp \left(-s \sum_{\mathbf{y} \in \Phi \setminus \{\mathbf{x}_c\}} h_{\mathbf{y}} \|\mathbf{y}\|^{-\alpha} \right) \mid n(\Phi) > 0 \right\} \\
&= \mathbb{E} \left\{ \prod_{\mathbf{y} \in \Phi \setminus \{\mathbf{x}_c\}} \exp \left(-s h_{\mathbf{y}} \|\mathbf{y}\|^{-\alpha} \right) \mid n(\Phi) > 0 \right\} \\
&\stackrel{(a)}{=} \mathbb{E} \left\{ \prod_{\mathbf{y} \in \Phi \setminus \{\mathbf{x}_c\}} \frac{1}{1 + s \|\mathbf{y}\|^{-\alpha}} \mid n(\Phi) > 0 \right\} \\
&\stackrel{(b)}{=} \exp \left(-\lambda \int_{\mathcal{A} \setminus \mathbf{b}(\mathbf{o}, R_c)} \left(1 - \frac{1}{1 + s \|\mathbf{y}\|^{-\alpha}} \right) d\mathbf{y} \right), \quad (18)
\end{aligned}$$

where (a) is found by $h_{\mathbf{y}} \sim \exp(1)$ and (b) follows from the PGFL of the PPP [4, Thm. 4.9] and the fact that interfering nodes are farther away than R_c . There are two types for $d < D$ (Case 1) and two types for $d > D$ (Case 2) to convert the result in (18) from Cartesian to polar coordinates. Each type denotes a special form of $\mathcal{A} \setminus \mathbf{b}(\mathbf{o}, R_c)$ that can be represented by polar coordinates uniquely.

Case 1:

Type 1: If $\mathcal{A} \cap \mathbf{b}(\mathbf{o}, R_c) = \mathbf{b}(\mathbf{o}, R_c)$ as given in Fig. 2(b), i.e., $0 \leq R_c < D - d$, then

$$\begin{aligned}
\mathcal{L}_{\mathcal{I}_c}^d(s|R_c) &= \exp \left(-\lambda \int_0^{2\pi} \int_0^{R_1(\theta)} \left(1 - \frac{1}{1 + sx^{-\alpha}} \right) x dx d\theta \right. \\
&\quad \left. + \lambda \int_0^{2\pi} \int_0^{R_c} \left(1 - \frac{1}{1 + sx^{-\alpha}} \right) x dx d\theta \right). \quad (19)
\end{aligned}$$

We can simplify (19) as

$$\begin{aligned}
\mathcal{L}_{\mathcal{I}_c}^d(s|R_c) &= \exp \left(2\pi\lambda \int_0^{R_c} \frac{x}{1 + \frac{x^\alpha}{s}} dx \right. \\
&\quad \left. - \lambda \int_0^{2\pi} \int_0^{R_1(\theta)} \frac{x}{1 + \frac{x^\alpha}{s}} dx d\theta \right) \\
&\stackrel{(c)}{=} \exp \left(\pi\lambda \mathcal{F}(s, R_c) - \lambda \int_0^\pi \mathcal{F}(s, R_1(\theta)) d\theta \right), \quad (20)
\end{aligned}$$

where (c) follows from replacing x^α with u and calculating the corresponding integral based on the formula [10, (3.194.1)] which uses the Gauss hypergeometric function.

Type 2: If $\mathcal{A} \cap \mathbf{b}(\mathbf{o}, R_c) \neq \mathbf{b}(\mathbf{o}, R_c)$ as given in Fig. 2(a), i.e., $D - d \leq R_c < D + d$, then

$$\begin{aligned}
& \mathcal{L}_{\mathcal{I}_c}^d(s|R_c) \\
&= \exp \left(-\lambda \int_{-\varphi_1(R_c)}^{\varphi_1(R_c)} \int_{R_c}^{R_1(\theta)} \left(1 - \frac{1}{1 + sx^{-\alpha}} \right) x dx d\theta \right) \\
&= \exp \left(-\lambda \int_0^{\varphi_1(R_c)} \left\{ \mathcal{F}(s, R_1(\theta)) - \mathcal{F}(s, R_c) \right\} d\theta \right). \quad (21)
\end{aligned}$$

Case 2: As observed from Fig. 2(c) for the case $d > D$, we have two different types of the LT of the interference

depending on whether or not the lower boundary of \mathcal{A} within the two tangent lines crossing the origin is included in the boundary of $\mathcal{A} \setminus \mathbf{b}(\mathbf{o}, R_c)$.

Type 1: Since the intersection angle $\varphi_1(r)$ at $r = \sqrt{d^2 - D^2}$ is equal to the angle of the tangent lines φ_0 , if $d - D < R_c < \sqrt{d^2 - D^2}$, then

$$\begin{aligned}
& \mathcal{L}_{\mathcal{I}_c}^d(s|R_c) = \\
& \exp \left(-\lambda \left\{ \int_{-\varphi_0}^{-\varphi_1(R_c)} \int_{\hat{R}_1(\theta)}^{R_1(\theta)} \left(1 - \frac{1}{1 + sx^{-\alpha}} \right) x dx d\theta \right. \right. \\
& \quad \left. \left. + \int_{-\varphi_1(R_c)}^{\varphi_1(R_c)} \int_{R_c}^{R_1(\theta)} \left(1 - \frac{1}{1 + sx^{-\alpha}} \right) x dx d\theta \right. \right. \\
& \quad \left. \left. + \int_{\varphi_1(R_c)}^{\varphi_0} \int_{\hat{R}_1(\theta)}^{R_1(\theta)} \left(1 - \frac{1}{1 + sx^{-\alpha}} \right) x dx d\theta \right\} \right) \\
&= \exp \left(-\lambda \int_{\varphi_1(R_c)}^{\varphi_0} \left\{ \mathcal{F}(s, R_1(\theta)) - \mathcal{F}(s, \hat{R}_1(\theta)) \right\} d\theta \right. \\
& \quad \left. - \lambda \int_0^{\varphi_1(R_c)} \left\{ \mathcal{F}(s, R_1(\theta)) - \mathcal{F}(s, R_c) \right\} d\theta \right). \quad (22)
\end{aligned}$$

Type 2: If $\sqrt{d^2 - D^2} < R_c < d + D$, then

$$\begin{aligned}
& \mathcal{L}_{\mathcal{I}_c}^d(s|R_c) \\
&= \exp \left(-\lambda \int_{-\varphi_1(R_c)}^{\varphi_1(R_c)} \int_{R_c}^{R_1(\theta)} \left(1 - \frac{1}{1 + sx^{-\alpha}} \right) x dx d\theta \right) \\
&= \exp \left(-\lambda \int_0^{\varphi_1(R_c)} \left\{ \mathcal{F}(s, R_1(\theta)) - \mathcal{F}(s, R_c) \right\} d\theta \right). \quad (23)
\end{aligned}$$

REFERENCES

- [1] J. G. Andrews, S. Buzzi, W. Choi, S. Hanly, A. Lozano, A. C. K. Soong, and J. C. Zhang, "What will 5G be?," *IEEE J. Sel. Areas Commun.*, vol. 32, no. 6, pp. 1065-1082, Jun. 2014.
- [2] M. Peng, C. Wang, V. Lau, and H. V. Poor, "Fronthaul-constrained cloud radio access networks: insights and challenges," *IEEE Wireless Commun.*, vol. 22, no. 2, pp. 152-160, April 2015.
- [3] M. Haenggi, J. G. Andrews, F. Baccelli, O. Dousse, and M. Franceschetti, "Stochastic geometry and random graphs for the analysis and design of wireless networks," *IEEE J. Sel. Areas Commun.*, vol. 27, no. 7, pp. 1029-1046, Sep. 2009.
- [4] M. Haenggi, *Stochastic Geometry for Wireless Networks*. Cambridge University Press, 2012.
- [5] M. Afshang and H. S. Dhillon, "Fundamentals of Modeling Finite Wireless Networks using Binomial Point Process", *IEEE Trans. Wireless Commun.*, vol. 16, no. 5, pp. 3355-3370, May 2017.
- [6] V. V. Chetlur and H. S. Dhillon, "Downlink Coverage Analysis for a Finite 3D Wireless Network of Unmanned Aerial Vehicles", *IEEE Trans. Commun.*, vol. 65, no. 10, pp. 4543-4558, July 2017.
- [7] J. Guo, S. Durrani, and X. Zhou, "Outage probability in arbitrarily-shaped finite wireless networks," *IEEE Trans. Commun.*, vol. 62, no. 2, pp. 699-712, Feb. 2014.
- [8] J. Guo, S. Durrani, and X. Zhou, "Performance analysis of arbitrarily-shaped underlay cognitive networks: Effects of secondary user activity protocols," *IEEE Trans. Commun.*, vol. 63, no. 2, pp. 376-389, Feb. 2015.
- [9] Z. Han and K. Liu, *Resource Allocation for Wireless Networks: Basics, Techniques, and Applications*. Cambridge University Press, 2008.
- [10] I. S. Gradshteyn and I. M. Ryzhik, *Table of Integrals, Series, and Products, 7th ed.* Academic Press, 2007.
- [11] J. G. Andrews, F. Baccelli, and R. K. Ganti, "A tractable approach to coverage and rate in cellular networks," *IEEE Trans. Commun.*, vol. 59, no. 11, pp. 3122-3134, Nov. 2011.